A Fast State Estimator for Systems Including Limited Number of PMUs

Ting Wu, *Student Member*, *IEEE*, C.Y. Chung, *Fellow*, *IEEE*, Innocent Kamwa, *Fellow, IEEE*

***Abstract*—This paper presents a fast state estimator and a corresponding bad data (BD) processing architecture aimed at improving computational efficiency and maintaining high estimation accuracy of existing state estimation (SE) algorithms, simultaneously. The conventional and phasor measurements are separately processed by a three-stage SE method and a linear estimator, respectively. Then, the derived estimates are combined using estimation fusion theory. To eliminate computational bottlenecks of the conventional BD processing scheme, BD identification is moved before the second stage of SCADA-based SE, and bad phasor measurements or bad conventional measurements in the PMU-observable area are identified and processed all at once, which can dramatically reduce the implementation time, especially for large-scale networks with multiple BD. The proposed estimator is compared to existing methods in terms of estimation accuracy and computational effort through simulation studies conducted on standard IEEE test systems. Promising simulation results show that the proposed estimator could be an effective method to obtain system states in a fast and accurate manner.**

***Index Terms*—State estimation, linear weighted least squares, phasor measurement unit, bad data processing, estimation fusion.**

I. INTRODUCTION

SINCE its initial introduction by Fred Schweppe in 1970 [1], state estimation (SE) has become an essential tool for providing accurate system snapshots to several crucial applications in energy management systems (EMS). The conventional SE [2], traditionally formulated as a nonlinear weighted least squares (WLS) problem and solved in an iterative manner, processes measurements obtained from the supervisory control and data acquisition (SCADA) system. With the increasing use of synchronized phasor measurement units (PMUs) in recent years, the measurement redundancy and estimation accuracy have been significantly improved because PMUs can provide synchronized voltage and current phasors with respect to the time reference obtained from the global positioning system (GPS) [3]. When a power system is fully observable using only PMU measurements, and rectangular coordinates are used for phasor measurements and state variables, the estimation problem becomes linear and can be non-iteratively solved [4]. Despite the undisputed advantages of using PMUs in power system SE, due to the financial constraints the number of PMUs deployed in real systems worldwide is still insufficient to make the system fully observable [5]. Moreover, the significant past investment in SCADA infrastructure can provide valuable information that should not simply be discarded. Thus, SCADA and PMU measurements will coexist for several years to come, and the power system SE should effectively integrate both of these available data sources and provide a unified view [6], [7]. To address the SE problem under incomplete PMU observability, two basic approaches, characterized structurally by the number of estimators used, are addressed: 1) mixing the SCADA and PMU measurements using a single estimator [5], [8]-[12]; and 2) processing each set of measurements separately and using two or more estimators [4], [6], [13]-[20]. Although the former approach can produce estimates with high accuracy, it faces some serious implementation challenges. One such challenge is caused by the significant difference between the refresh rates of SCADA and PMU measurements, which can be successfully circumvented by the latter approach.

Even though computing power is now orders of magnitude greater than four decades ago, when power system SE was championed by Schweppe, the need for computationally more efficient techniques to integrate data from both the SCADA system and PMUs still remains due to expansion of the geographical scope of many SEs and the huge number of measurement points provided by the ongoing deployment of new digital devices [21], [22]. A reduced-order two-stage method, proposed in [4] to perform SE using both SCADA and PMU measurements, featured lower computational complexity. To reduce the required execution time, the authors in [13] offered an alternative approach to incorporate PMU data into conventional SE through a post-processing step. This scheme was modified in [15] by introducing supplementary current measurements in the post-processing step to provide slightly higher precision. A two-stage state estimator was proposed in [16] to reduce computational effort. A distributed SE algorithm was presented in [17] and the simulation results demonstrated its efficacy in reducing the computational time. A distributed two-level state estimator function [19], [20] used a linear SE

This work was supported in part by the Department of Electrical Engineering of The Hong Kong Polytechnic University, the College of Information Engineering of Zhejiang University of Technology, the Department of Electrical and Computer Engineering of the University of Saskatchewan, Hydro-Québec's research institute, and the Natural Sciences and Engineering Research Council (NSERC) of Canada.

T. Wu is with the College of Information Engineering, Zhejiang University of Technology, Hangzhou 310023, China, and also with the Department of Electrical Engineering, The Hong Kong Polytechnic University, Hong Kong. (e-mail: twu920@gmail.com)

C.Y. Chung is with the Department of Electrical and Computer Engineering, University of Saskatchewan, Saskatoon, SK S7N 5A9 Canada. (e-mail: c.y.chung@usask.ca).

I. Kamwa is with the Hydro-Québec/IREQ, Power System and Mathematics, Varennes QC J3X 1S1, Canada (e-mail: kamwa.innocent@ireq.ca)

algorithm at the control center level but moved the bad data identification and local topology processing to the substation level, making this processing very fast.

Bad data (BD) analysis is an essential attribute of any power system state estimator, and a variety of methods for gross error detection and identification are available. Among existing methods, the largest normalized residual test [2] and the hypothesis testing identification (HTI) method [23] are widely used for SCADA-based SE. With the increasing penetration of PMUs in power system SE, BD analysis in PMU measurements has been a matter of interest for several years. A strategic PMU placement algorithm was proposed in [24] to improve the BD processing capability of state estimators. The authors in [10] applied the largest normalized residual test to address BD analysis in the context of hybrid SE. However, for multiple BD, updates on the measurements and states continue until all normalized residuals drop below a pre-defined detection threshold. Thus, the re-estimation step constitutes the main computational bottleneck of the BD analysis. To efficiently identify multiple gross errors and eliminate a BD smearing effect, an enhanced BD processing approach was developed in [7]. However, computational burden associated with the nonlinear re-estimation step of SCADA-based SE may lower its performance when there are multiple bad SCADA measurements in PMU-unobservable area. Therefore, there is a need to develop a new SE algorithm to improve computational efficiency which is crucial not only for the solution but also for the BD processing scheme.

The focus of this paper is on developing a new SE method to improve computational efficiency and maintain high estimation accuracy simultaneously, especially for large-scale networks with multiple BD. First, a three-stage SE method, composed of two WLS linear problems and a nonlinear transformation, is used to process the SCADA data. Then, the PMU observable states are calculated by a linear estimator, whereas pseudo state values with large variances are assigned to PMU unobservable states. A fusion stage is used to combine the results obtained from the above two estimators. Bad SCADA measurements in PMU-observable area or bad PMU measurements are identified and processed all at once, which can dramatically reduce the implementation time. In addition, the linear re-estimation step, caused by bad SCADA measurements in PMU-unobservable area, can further improve computational efficiency.

The rest of this paper is organized as follows. Section II presents the proposed state estimator and bad data processing scheme. In Section III, the solution accuracy and computational effort of the proposed algorithm are compared to existing methods using the IEEE 14-, 30-, 57-, 118-, and 300-bus test systems. Finally, Section IV provides conclusions.

II. Proposed State Estimation

This section describes a fast state estimator for integrating SCADA and PMU measurements. Consider a power system with n buses, l branches, and measured by m_s SCADA measurements and m_p PMU measurements.

A. First Stage of SCADA-Based SE

In the first stage, an auxiliary vector, y, is introduced in such a way that a linear measurement model is represented by [21]

$$z_{\text{scada}} = Ay + e_1 \quad (1)\#$$

where z_{scada} is the SCADA measurement vector with dimension ($m_s\times 1$); A is a constant Jacobian matrix; and e_1 is the measurement error vector that features a normal distribution with zero mean and covariance matrix R_{SCADA}.

Specifically, for each bus i, the voltage magnitude V_i is squared to get the new variable U_i:

$$U_i = V_i^2 . \quad (2)\#$$

Moreover, for each branch connecting buses i and j, the following two variables are constructed:

$$K_{ij} = V_i V_j \cos\theta_{ij} \quad (3)\#$$

$$L_{ij} = V_i V_j \sin\theta_{ij} \quad (4)\#$$

where θ_i and θ_j denote the voltage phase angles of buses i and j, respectively, and $\theta_{ij} = \theta_i - \theta_j$.

Then, the intermediate state vector, composed of n+2l variables, is given in block partitioned form:

$$y = \left\{ U_i \quad K_{ij} \quad L_{ij} \right\} . \quad (5)\#$$

Any SCADA measurement can be linearly expressed in terms of the intermediate state vector as follows [21].

- *Power flow measurements*

For a branch connecting buses i and j, active and reactive power flow measurements taken at terminal bus i are

$$P_{ij} = (g_{sh,i} + g_{ij})U_i - g_{ij}K_{ij} - b_{ij}L_{ij} + \varepsilon_P \quad (6)\#$$

$$Q_{ij} = -(b_{sh,i} + b_{ij})U_i + b_{ij}K_{ij} - g_{ij}L_{ij} + \varepsilon_Q \quad (7)\#$$

where g_{ij} and b_{ij} are the conductance and susceptance of the series branch connecting buses i and j, respectively, and $g_{sh,i}$ and $b_{sh,i}$ are the values of the shunt branch connected at bus i.

- *Power injection measurements at bus i*

$$P_i = \sum_{j\in i} P_{ij} + \varepsilon_P \quad (8)\#$$

$$Q_i = \sum_{j\in i} Q_{ij} + \varepsilon_Q . \quad (9)\#$$

- *Voltage magnitude measurement*

Here, the voltage magnitude measurements should be squared to retain linearity in this stage:

$$V_i^2 = U_i + \varepsilon_U . \quad (10)$$

The standard deviation of the error associated with V_i^2 is calculated using the original measurement V_i and its standard deviation, as follows:

$$\sigma\left(V_i^2\right) = 2V_i\sigma\left(V_i\right) . \quad (11)\#$$

The components of constant Jacobian matrix A in (1) are given in [21] and [22]. The WLS solution to the linear problem (1), $\hat{y}^{(\text{scada})}$, and its error covariance matrix, $R_y^{(\text{scada})}$, can be directly obtained, respectively, as:

$$\hat{y}^{(\text{scada})} = G_a^{-1} A^{\mathrm{T}} R_{\text{SCADA}}^{-1} z_{\text{scada}} \quad (12)$$

$$R_y^{(\text{scada})} = G_a^{-1} \quad (13)\#$$

where $G_a = A^{\mathrm{T}} R_{\text{SCADA}}^{-1} A$ is a gain matrix and the notation $(\cdot)^{\mathrm{T}}$ denotes transpose.

B. PMU-Based SE

PMUs offer fast acquisition of voltage and current phasors in a synchronized manner. When rectangular coordinates are used for the phasor measurements and state variables, the SE problem becomes linear and states can be obtained by a non-iterative algorithm. However, the phasor measurements derived from PMUs are generally stored and uploaded in polar form. The relationship between incremental representation in polar and rectangular coordinates is

$$\begin{aligned}&\begin{bmatrix} z_{(1)\mathrm{re}} & z_{(2)\mathrm{re}} & \cdots & z_{(1)\mathrm{im}} & z_{(2)\mathrm{im}} & \cdots \end{bmatrix}^{\mathrm{T}} = \\ &T_{\mathrm{PMU}} \begin{bmatrix} \Delta\theta_1 & \Delta\theta_2 & \cdots & \Delta|z_1| & \Delta|z_2| & \cdots \end{bmatrix}^{\mathrm{T}}\end{aligned} \tag{14}$$

where

$$T_{\mathrm{PMU}} = \begin{bmatrix} -|z_1|\sin\theta_1 & 0 & \cdots & \cos\theta_1 & 0 & \cdots \\ 0 & -|z_2|\sin\theta_2 & \cdots & 0 & \cos\theta_2 & \cdots \\ \vdots & \vdots & \cdots & \vdots & \vdots & \cdots \\ |z_1|\cos\theta_1 & 0 & \cdots & \sin\theta_1 & 0 & \cdots \\ 0 & |z_2|\cos\theta_2 & \cdots & 0 & \sin\theta_2 & \cdots \\ \vdots & \vdots & \cdots & \vdots & \vdots & \cdots \end{bmatrix}$$

$z_{(1)\mathrm{re}}$ and $z_{(1)\mathrm{im}}$ represent the rectangular form of PMU measurements, and $|z_1|$ and θ_1 denote their polar form. The error covariance matrix of the measurements in polar coordinates, $R_{\mathrm{PMU}}^{\mathrm{p}}$, is thereby transformed by a rotation matrix T_{PMU} to obtain the error covariance matrix of measurements in rectangular coordinates, $R_{\mathrm{PMU}}^{\mathrm{r}}$:

$$R_{\mathrm{PMU}}^{\mathrm{r}} = T_{\mathrm{PMU}} R_{\mathrm{PMU}}^{\mathrm{p}} \left(T_{\mathrm{PMU}}\right)^{\mathrm{T}}. \tag{15}$$

After the above transformation, a set of positive sequence voltage and current phasors in rectangular coordinates, z_{pmu}, is obtained. PMU observable states are uniquely defined by the PMU placements and the type of PMU measurements [4]. We assume there are n_{ob} PMU observable states and n_{un} PMU unobservable states, which are denoted by x_{ob} and x_{un} respectively. A permutation matrix Π is easily defined to reorder the state vector x such that the PMU observable states are stacked over the unobservable states, i.e., $\Pi x = \begin{bmatrix} x_{\mathrm{ob}}^{\mathrm{T}} & x_{\mathrm{un}}^{\mathrm{T}} \end{bmatrix}^{\mathrm{T}}$. Because $\Pi^{\mathrm{T}}\Pi = I$, the PMU measurement model can be expressed as follows:

$$z_{\mathrm{pmu}} = Bx + e_2 = B\Pi^{\mathrm{T}}\Pi x + e_2 = \begin{bmatrix} C_1 & C_2 \end{bmatrix} \begin{bmatrix} x_{\mathrm{ob}} \\ x_{\mathrm{un}} \end{bmatrix} + e_2 \tag{16}$$#

where B is the PMU measurement Jacobian, with dimension ($m_{\mathrm{p}} \times 2n$), and $B\Pi^{\mathrm{T}} = \begin{bmatrix} C_1 & C_2 \end{bmatrix}$. The dimensions of C_1 and C_2 are $m_{\mathrm{p}} \times n_{\mathrm{ob}}$ and $m_{\mathrm{p}} \times n_{\mathrm{un}}$, respectively. Because all entries in C_2 are zero, (16) can be rewritten as

$$z_{\mathrm{pmu}} = C_1 x_{\mathrm{ob}} + e_2. \tag{17}$$#

Then, the estimate for the PMU observable state vector and its error covariance are given, respectively, by:

$$\hat{x}_{\mathrm{ob}} = \left[C_1^{\mathrm{T}} \left(R_{\mathrm{PMU}}^{r} \right)^{-1} C_1 \right]^{-1} C_1^{\mathrm{T}} \left(R_{\mathrm{PMU}}^{r} \right)^{-1} z_{\mathrm{pmu}} \tag{18}$$#

$$R_{\mathrm{ob}} = \left[C_1^{\mathrm{T}} \left(R_{\mathrm{PMU}}^{r} \right)^{-1} C_1 \right]^{-1}. \tag{19}$$#

In preparation for bad data processing and the fusion stage, standard "expected" values for bus complex voltages (real part = 1, imaginary part = 0) are assigned to the PMU-unobservable state vector $\hat{x}_{\mathrm{un}}$. Because these PMU-unobservable state values are inaccurate, their variances are usually some orders of magnitude larger than the tele-measurement variances. Let R_{un} ($n_{\mathrm{un}} \times n_{\mathrm{un}}$ diagonal matrix) be the error covariance matrix of $\hat{x}_{\mathrm{un}}$. Then, the estimate for the state vector $\hat{x}^{(\mathrm{pmu})}$ and its error covariance matrix $R_x^{(\mathrm{pmu})}$ are calculated using

$$\hat{x}^{(\mathrm{pmu})} = \Pi^{\mathrm{T}} \begin{bmatrix} \hat{x}_{\mathrm{ob}} \\ \hat{x}_{\mathrm{un}} \end{bmatrix} \tag{20}$$#

$$R_x^{(\mathrm{pmu})} = \Pi_1^{\mathrm{T}} R_{\mathrm{ob}} \Pi_1 + \Pi_2^{\mathrm{T}} R_{\mathrm{un}} \Pi_2 \tag{21}$$#

where $\Pi = \begin{bmatrix} \Pi_1^{\mathrm{T}} & \Pi_2^{\mathrm{T}} \end{bmatrix}^{\mathrm{T}}$, and the dimensions of Π_1 and Π_2 are $n_{\mathrm{ob}} \times 2n$ and $n_{\mathrm{un}} \times 2n$, respectively.

C. Bad Data Processing Scheme

The previous two subsections process SCADA and PMU measurements independently and individually. When "scada" and "pmu" are used as superscripts, they denote in which estimator a vector/matrix is computed, whereas subscripts "scada" and "pmu" represent the type of measurements to which a vector/matrix is associated [7].

The state estimate $\hat{x}^{(\mathrm{pmu})}$ is obtained together with its error covariance matrix $R_x^{(\mathrm{pmu})}$ from processing PMU measurements only. Then, using $\hat{x}^{(\mathrm{pmu})}$, the estimated intermediate state vector $\hat{y}^{(\mathrm{pmu})}$ is calculated as follows:

$$\hat{y}^{(\mathrm{pmu})} = \left\{ \hat{U}_i^{(\mathrm{pmu})} \quad \hat{K}_{ij}^{(\mathrm{pmu})} \quad \hat{L}_{ij}^{(\mathrm{pmu})} \right\} \tag{22}$$

where

$$\hat{U}_i^{(\mathrm{pmu})} = \left(\hat{x}_{(i)\mathrm{re}}^{(\mathrm{pmu})} \right)^2 + \left(\hat{x}_{(i)\mathrm{im}}^{(\mathrm{pmu})} \right)^2 \tag{23}$$

$$\hat{K}_{ij}^{(\mathrm{pmu})} = \hat{x}_{(i)\mathrm{re}}^{(\mathrm{pmu})} \hat{x}_{(j)\mathrm{re}}^{(\mathrm{pmu})} + \hat{x}_{(i)\mathrm{im}}^{(\mathrm{pmu})} \hat{x}_{(j)\mathrm{im}}^{(\mathrm{pmu})} \tag{24}$$

$$\hat{L}_{ij}^{(\mathrm{pmu})} = \hat{x}_{(i)\mathrm{im}}^{(\mathrm{pmu})} \hat{x}_{(j)\mathrm{re}}^{(\mathrm{pmu})} - \hat{x}_{(i)\mathrm{re}}^{(\mathrm{pmu})} \hat{x}_{(j)\mathrm{im}}^{(\mathrm{pmu})} \tag{25}$$

where $\hat{x}_{(i)\mathrm{re}}^{(\mathrm{pmu})}$ and $\hat{x}_{(i)\mathrm{im}}^{(\mathrm{pmu})}$ are the real and imaginary parts of the estimated voltage phasor for bus I, respectively, which are obtained from (20). From the above relationships (23)-(25), the $(n+2l)\times 2n$ Jacobian $F_y = \partial y / \partial x$ is evaluated at $x = \hat{x}^{(\mathrm{pmu})}$, and its components are provided in Table I.

TABLE I
JACOBIAN COMPONENTS IN THE BD PROCESSING SCHEME

	$x = x_{(i)\mathrm{re}}$	$x = x_{(i)\mathrm{im}}$	$x = x_{(j)\mathrm{re}}$	$x = x_{(j)\mathrm{im}}$
$\partial U_i / \partial x$	$2x_{(i)\mathrm{re}}$	$2x_{(i)\mathrm{im}}$	0	0
$\partial K_{ij} / \partial x$	$x_{(j)\mathrm{re}}$	$x_{(j)\mathrm{im}}$	$x_{(i)\mathrm{re}}$	$x_{(i)\mathrm{im}}$
$\partial L_{ij} / \partial x$	$-x_{(j)\mathrm{im}}$	$x_{(j)\mathrm{re}}$	$x_{(i)\mathrm{im}}$	$-x_{(i)\mathrm{re}}$

Therefore, the error covariance matrix of $\hat{y}^{(\mathrm{pmu})}$ is calculated as

$$R_y^{(\mathrm{pmu})} = F_y R_x^{(\mathrm{pmu})} F_y^{\mathrm{T}}. \tag{26}$$#

Using $\hat{y}^{(\mathrm{pmu})}$, the estimated SCADA measurement vector $\hat{z}_{\mathrm{scada}}^{(\mathrm{pmu})}$ and its error covariance matrix $M_{\mathrm{scada}}^{(\mathrm{pmu})}$ are given by

$$\hat{z}_{\mathrm{scada}}^{(\mathrm{pmu})} = A\hat{y}^{(\mathrm{pmu})} \tag{27}$$#

$$M_{\mathrm{scada}}^{(\mathrm{pmu})} = AR_y^{(\mathrm{pmu})} A^{\mathrm{T}}. \tag{28}$$#

Thus, considering the SCADA measurement vector z_{scada}, the following difference vector and its covariance matrix are computed, respectively, as [7]

$$r_{\text{scada}}^{(\text{pmu})} = z_{\text{scada}} - \hat{z}_{\text{scada}}^{(\text{pmu})} \quad (29)\#$$

$$J_{\text{scada}}^{(\text{pmu})} = R_{\text{SCADA}} + M_{\text{scada}}^{(\text{pmu})} . \quad (30)\#$$

The components of $r_{\text{scada}}^{(\text{pmu})}$ are normalized as follows:

$$r_{N\text{scada}}^{(\text{pmu})}(i) = \frac{r_{\text{scada}}^{(\text{pmu})}(i)}{\sqrt{J_{\text{scada}}^{(\text{pmu})}(i,i)}} . \quad (31)$$

A flag vector α with the same dimension as z_{scada} is defined as#

$$\alpha(i) = \begin{cases} 0, & r_{N\text{scada}}^{(\text{pmu})}(i) \le \text{threshold} \\ 1, & r_{N\text{scada}}^{(\text{pmu})}(i) > \text{threshold} \end{cases} . \quad (32)\#$$

Similarly, $\hat{y}^{(\text{scada})}$ is used to calculate the estimated SCADA measurement vector $\hat{z}_{\text{scada}}^{(\text{scada})}$ and its error covariance matrix $M_{\text{scada}}^{(\text{scada})}$, respectively, using

$$\hat{z}_{\text{scada}}^{(\text{scada})} = A\hat{y}^{(\text{scada})} \quad (33)\#$$

$$M_{\text{scada}}^{(\text{scada})} = AR_{y}^{(\text{scada})}A^{\text{T}} . \quad (34)\#$$

Then, the estimation residual vector and its covariance matrix are given by

$$r_{\text{scada}}^{(\text{scada})} = z_{\text{scada}} - \hat{z}_{\text{scada}}^{(\text{scada})} \quad (35)\#$$

$$J_{\text{scada}}^{(\text{scada})} = R_{\text{SCADA}} - M_{\text{scada}}^{(\text{scada})} . \quad (36)\#$$

The components of $r_{\text{scada}}^{(\text{scada})}$ are normalized as

$$r_{N\text{scada}}^{(\text{scada})}(i) = \frac{r_{\text{scada}}^{(\text{scada})}(i)}{\sqrt{J_{\text{scada}}^{(\text{scada})}(i,i)}} \quad (37)$$

and a flag vector β with the same size of z_{scada} is defined as

$$\beta(i) = \begin{cases} 0, & r_{N\text{scada}}^{(\text{scada})}(i) \le \text{threshold} \\ 1, & r_{N\text{scada}}^{(\text{scada})}(i) > \text{threshold} \end{cases} . \quad (38)\#$$

It is worth mentioning that the flag vector β is valid in the case of non-critical single or uncorrelated multiple BD.

Since only SCADA measurements are used in (33)-(38), the flag vector β just identifies the suspicious bad SCADA measurements. The diagnosis of BD should integrate the information from both flag vectors α and β as shown in Table II.

TABLE II
DIAGNOSIS OF BAD DATA

	Bad Data Indication	Diagnosis
1	$\text{sum}(\alpha) = 0$ & $\text{sum}(\beta) = 0$	No BD
2	$\text{sum}(\alpha) = 0$ & $\text{sum}(\beta) \ne 0$	BD in z_{scada} (all of these BD are in the PMU-unobservable area)
3	$\text{sum}(\alpha) \ne 0$ & $\text{sum}(\beta) \ne 0$	BD in z_{scada} (some/all of these BD are in the PMU-observable area)
4	$\text{sum}(\alpha) \ne 0$ & $\text{sum}(\beta) = 0$	BD in PMU measurements

We assume that BD in SCADA and PMU measurements do not occur simultaneously. ***Scenario 1:*** If flag vectors α and β are zero vectors, i.e., no threshold violations in either $r_{N\text{scada}}^{(\text{pmu})}$ or $r_{N\text{scada}}^{(\text{scada})}$, then there are no BD in the SCADA and PMU measurements. ***Scenario 2:*** In the case of threshold violations in $r_{N\text{scada}}^{(\text{scada})}$ indicated by the non-zero value of the sum of all components in flag vector β and no threshold violations in $r_{N\text{scada}}^{(\text{pmu})}$, bad SCADA measurements occur in the PMU-unobservable area. Then, the conventional BD processing method, i.e., repeated application of BD detection, identification, correction, and re-estimation, is performed to eliminate the BD one-by-one. As shown in (11), if a bad voltage magnitude measurement exists in the PMU-unobservable area, the variance of its squared version is corrupted and cannot be used in the correction step. Thus, the bad voltage magnitude measurements in this scenario should be deleted, whereas other bad SCADA measurements, such as active/reactive power flows and power injections, are corrected as follows:

$$z_{\text{scada}}^{\text{new}}(i) = z_{\text{scada}}^{\text{bad}}(i) - \frac{R_{\text{SCADA}}(i,i)}{J_{\text{scada}}^{(\text{scada})}(i,i)} r_{\text{scada}}^{(\text{scada})}(i) . \quad (39)$$

Scenario 3: Non-zero vectors α and β indicate the presence of gross errors in z_{scada}, and some or all of these BD occur within the network area observed by PMU measurements. First, the suspect SCADA measurements flagged by α can easily be replaced all at once by their corresponding estimates obtained from (27), weighted according to the diagonal elements of matrix $M_{\text{scada}}^{(\text{pmu})}$ defined in (28). The intermediate state vector y is then re-estimated using the updated SCADA measurements. Lastly, the normalized estimation residual vector is re-calculated to check whether there are still bad SCADA measurements in the PMU-unobservable area. If elements in $r_{N\text{scada}}^{(\text{scada})}$ exceed the predefined threshold, the bad SCADA measurements can only be eliminated one-by-one using a conventional BD processing scheme, as in Scenario 2. ***Scenario 4:*** If zero vector β validates SCADA measurements but elements of $r_{N\text{scada}}^{(\text{pmu})}$ exceed the detection threshold, one can conclude that the estimated measurement $\hat{z}_{\text{scada}}^{(\text{pmu})}$ obtained in (27) is contaminated by the presence of BD in PMU measurements. In this situation, $\hat{y}^{(\text{scada})}$ obtained in (12) is valid and can be used to obtain state vector $\hat{x}^{(\text{scada})}$ (in rectangular form) and its error covariance matrix $R_{x}^{(\text{scada})}$ as per Section II-D. Then, the estimated PMU measurements $\hat{z}_{\text{pmu}}^{(\text{scada})}$ and the error covariance matrix $M_{\text{pmu}}^{(\text{scada})}$ are given by

$$\hat{z}_{\text{pmu}}^{(\text{scada})} = B\hat{x}^{(\text{scada})} \quad (40)\#$$

$$M_{\text{pmu}}^{(\text{scada})} = BR_{x}^{(\text{scada})}B^{\text{T}} . \quad (41)\#$$

Similarly, the following differences can be computed, normalized, and flagged:

$$r_{\text{pmu}}^{(\text{scada})} = z_{\text{pmu}} - \hat{z}_{\text{pmu}}^{(\text{scada})} \quad (42)\#$$

$$J_{\text{pmu}}^{(\text{scada})} = R_{\text{PMU}}^{\text{r}} + M_{\text{pmu}}^{(\text{scada})} \quad (43)\#$$

$$r_{N\text{pmu}}^{(\text{scada})}(i) = \frac{r_{\text{pmu}}^{(\text{scada})}(i)}{\sqrt{J_{\text{pmu}}^{(\text{scada})}(i,i)}} \quad (44)$$

$$\gamma(i) = \begin{cases} 0, & r_{N\text{pmu}}^{(\text{scada})}(i) \le \text{threshold} \\ 1, & r_{N\text{pmu}}^{(\text{scada})}(i) > \text{threshold} \end{cases} . \quad (45)\#$$

Compared to tele-measurement, the estimated PMU measurements $\hat{z}_{\text{pmu}}^{(\text{scada})}$ are not sufficiently accurate. Furthermore, as shown in (14) and (15), the covariance matrix

$R^{\mathrm{r}}_{\mathrm{PMU}}$ is contaminated if there are BD in PMU measurements and therefore cannot be used to correct the BD in the hybrid estimator [10] and the alternative estimator [13] mentioned in the next section. Thus, instead of replacing the BD by their estimates obtained in (40), the spurious PMU measurements flagged by the vector γ are deleted all at once. The block diagram depicted in Fig. 1 represents the proposed SE and BD processing scheme. The PMU-based SE and the first stage of SCADA-based SE are processed in parallel.

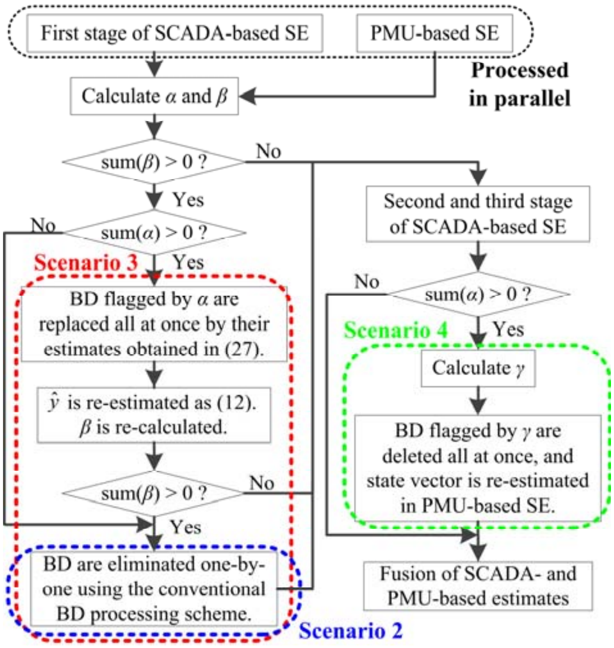

Fig. 1. Architecture of proposed SE and BD processing scheme.

D. Second and Third Stages of SCADA-Based SE

So far, we can confirm no BD in the SCADA measurements. The state vector is computed through the second and third stages of SCADA-based SE as follows.

To obtain a new vector u that is, in turn, linearly related to the conventional state vector, an explicit nonlinear transformation, shown in (46), is applied to the estimate y provided by the first stage of SCADA-based SE [21]:

$$u = f_u(y)\ . \tag{46}$$

The components of vector u,

$$u = \left\{ \zeta_i \quad \zeta_{ij} \quad \theta_{ij} \right\}, \tag{47}$$

can be explicitly related to those of vector y as follows:

$$\zeta_i = \ln U_i \tag{48}$$

$$\zeta_{ij} = \ln\left(K_{ij}^2 + L_{ij}^2\right) \tag{49}$$

$$\theta_{ij} = \arctan\left(L_{ij} / K_{ij}\right). \tag{50}$$

From the above nonlinear relationships (48)-(50), the $(n+2l)\times(n+2l)$ Jacobian $F_u = \partial u/\partial y$ is evaluated at $y = \hat{y}^{(\mathrm{scada})}$, and its components are given as follows:

$$\partial\zeta_i / \partial U_i = 1/U_i \tag{51}$$

$$\begin{bmatrix} \partial\zeta_{ij}/\partial K_{ij} & \partial\zeta_{ij}/\partial L_{ij} \\ \partial\theta_{ij}/\partial K_{ij} & \partial\theta_{ij}/\partial L_{ij} \end{bmatrix} = \frac{1}{K_{ij}^2 + L_{ij}^2}\begin{bmatrix} 2K_{ij} & 2L_{ij} \\ -L_{ij} & K_{ij} \end{bmatrix}. \tag{52}$$

Then, the error covariance matrix of u is calculated as follows:

$$R_u = F_u R_y^{(\mathrm{scada})} F_u^{\mathrm{T}}\ . \tag{53}$$

In the final stage, the state vector s is slightly modified in such a way that u is a linear function thereof. For this purpose, u and s in blocked form are expressed as

$$u = [\zeta^{\mathrm{T}} \quad \zeta_b^{\mathrm{T}} \quad \theta_b^{\mathrm{T}}]^{\mathrm{T}}; \qquad s = [\zeta^{\mathrm{T}} \quad \theta^{\mathrm{T}}]^{\mathrm{T}}$$

where the subscript "b" denotes the set of branch variables, and logarithmic version ζ is chosen as the state rather than the ordinary voltage magnitude. Then, the linear measurement model in blocked form is given by

$$u = Ds + e_u \quad \Rightarrow \quad \begin{bmatrix} \zeta \\ \zeta_b \\ \theta_b \end{bmatrix} = \begin{bmatrix} I & 0 \\ |S^{\mathrm{T}}| & 0 \\ 0 & N^{\mathrm{T}} \end{bmatrix} \begin{bmatrix} \zeta \\ \theta \end{bmatrix} + e_u \tag{54}$$

where S is the branch-to-node incidence matrix and N is a reduced matrix obtained by omitting the reference phase angle in S. The WLS estimate $\hat{s}$ and its error covariance matrix can be computed as follows:

$$\hat{s} = G_{\mathrm{d}}^{-1} D^{\mathrm{T}} R_u^{-1} \hat{u} \tag{55}$$

$$R_s = G_{\mathrm{d}}^{-1} \tag{56}$$

where $G_{\mathrm{d}} = D^{\mathrm{T}} R_u^{-1} D$ is the gain matrix and $\hat{u}$ is obtained from (47)-(50). Once ζ in $\hat{s}$ is available, voltage magnitude $V = 0.5\exp(\zeta)$ can be readily obtained. Thus, the relationship between incremental representation of the state vector in polar form $x_{\mathrm{p}} = [V^{\mathrm{T}} \quad \theta^{\mathrm{T}}]^{\mathrm{T}}$ and the state vector in (54) is given by

$$\Delta x_{\mathrm{p}} = F_x \Delta s \quad \Rightarrow \quad \begin{bmatrix} \Delta V \\ \Delta\theta \end{bmatrix} = \begin{bmatrix} 0.5\exp(\zeta) & \\ & I \end{bmatrix} \begin{bmatrix} \Delta\zeta \\ \Delta\theta \end{bmatrix} \tag{57}$$

where Jacobian $F_x = \partial x/\partial s$ is evaluated at $s = \hat{s}$. The error covariance matrix of x_{p}, $R^{\mathrm{p}}_{\mathrm{SCADA}}$, is then

$$R^{\mathrm{p}}_{\mathrm{SCADA}} = F_x R_s F_x^{\mathrm{T}}\ . \tag{58}$$

To formulate the fusion step, $\hat{x}_{\mathrm{p}}$ should be transformed to achieve the state vector in rectangular coordinates $\hat{x}^{(\mathrm{scada})}$. Meanwhile, the error covariance matrix of $\hat{x}^{(\mathrm{scada})}$ is given by

$$R_x^{(\mathrm{scada})} = T_{\mathrm{SCADA}} R^{\mathrm{p}}_{\mathrm{SCADA}} \left(T_{\mathrm{SCADA}}\right)^{\mathrm{T}} \tag{59}$$

where rotation matrix T_{SCADA} is similar to that in (15) but different in detail and size.

E. Fusion of SCADA- and PMU-Based Estimates

The final state estimate, $x^{(\mathrm{final})}$, can be computed as [6]

$$\hat{x}^{(\mathrm{final})} = W_1 \hat{x}^{(\mathrm{scada})} + W_2 \hat{x}^{(\mathrm{pmu})} \tag{60}$$

where the weights in the above equation are given by

$$W_1 = R_x^{(\mathrm{pmu})} \left(R_x^{(\mathrm{scada})} + R_x^{(\mathrm{pmu})}\right)^{-1} \tag{61}$$

$$W_2 = R_x^{(\mathrm{scada})} \left(R_x^{(\mathrm{scada})} + R_x^{(\mathrm{pmu})}\right)^{-1}. \tag{62}$$

As mentioned in Section II-B, large variances are assigned to the PMU-unobservable states, so the estimates provided for those states in PMU-based SE receive very small weights. The corresponding SCADA-based estimates eventually prevail at the fusion step and the final estimates will not be contaminated by inaccurate PMU-unobservable states.

III. SIMULATION RESULTS

In this section, the simulation results corresponding to the IEEE 14-, 30-, 57-, 118-, and 300-bus test systems [25] are presented and discussed. Four distinct estimators are employed as references to evaluate the proposed fast SE method (FSE) in terms of solution accuracy and computational effort: a hybrid estimator (HSE) [10], a conventional SCADA-based estimator (SSE) [2], a bilinear SCADA-based estimator (BSE) [21], and an alternative estimator (ASE) developed in [13]. SSE and BSE only use the SCADA measurements, while the other three estimators integrate data from both the SCADA system and PMUs. Specifically, instead of performing the well-known Gauss-Newton iterative scheme in SSE [2], BSE is composed of two WLS linear models and a nonlinear explicit transformation in between [21]. Moreover, in the HSE formulation, PMU and SCADA measurements are simultaneously processed in a single non-linear WLS estimator [10], but ASE uses the PMU measurements through a linear post-processing step after obtaining the results of SSE [13]. So far, HSE is recognized as the best state estimator that incorporates both SCADA and PMU measurements in terms of accuracy [6], [7]. For SCADA measurements, unless otherwise noted, it is assumed that voltage measurements and power injections are taken at all buses, and power flows are taken across all branches ("from" terminal only). A PMU placed at a bus is assumed to measure the voltage phasor at that bus as well as the current phasors on all lines incident to that bus. The PMU placement configurations adopted in this study are documented in [4]. Table III gives the measurement types and the corresponding standard deviations used in this study. The variance of pseudo states used in Section II-B is 1×10^8.

TABLE III
STANDARD DEVIATIONS FOR SCADA AND PMU MEASUREMENTS

SCADA measurement			PMU measurements		
$\lvert V\rvert$	Power flows	Power injections	$\lvert V\rvert$	$\lvert I\rvert$	Phase angle
1%	2%	2%	0.1%	0.1%	0.0017 rad

A. Assessment of Estimation Accuracy

Figs. 2, 3, 4, and 5 illustrate the absolute estimation errors (averaged over 100 statistical trials) of five estimators associated with the estimates of the voltage phase angle and magnitude at each bus for the IEEE 14-bus, 30-bus, 57-bus, and 118-bus test systems, respectively (results for the 300-bus system are omitted due to space limitations). The FSE plot clearly shows that the limited PMU measurements can greatly enhance the results of the bilinear SCADA-based estimator, labeled as BSE, through a fusion stage. Moreover, FSE estimation errors are almost coincident with those of HSE, which demonstrates that the pseudo states with large variances used in PMU-based SE are filtered out in the fusion procedure and do not affect the final estimation results.

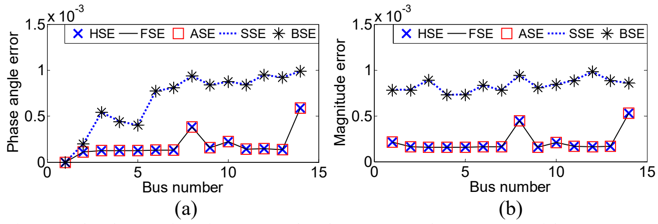

Fig. 2. Absolute estimation errors for the IEEE 14-bus system without BD: (a) voltage phase angle error and (b) voltage magnitude error.

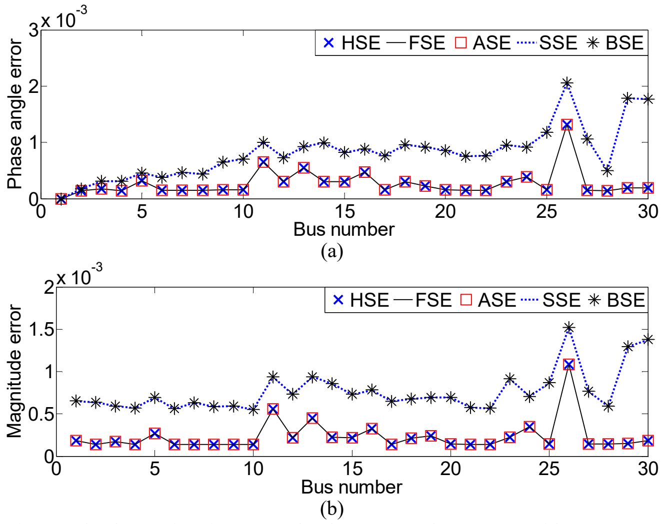

Fig. 3. Absolute estimation errors for the IEEE 30-bus system without BD: (a) voltage phase angle error and (b) voltage magnitude error.

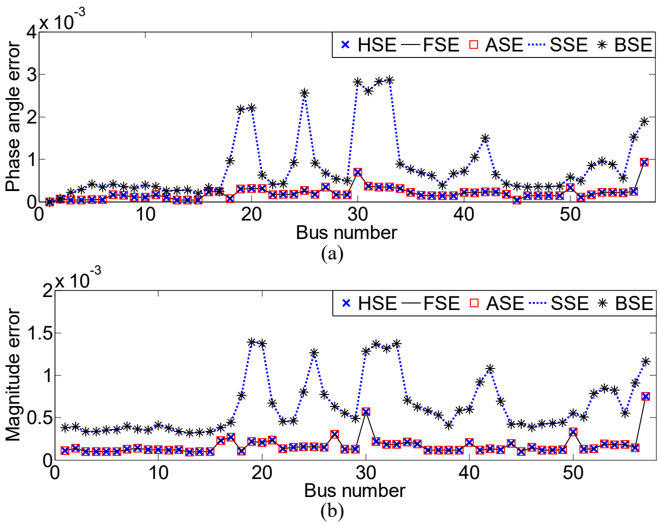

Fig. 4. Absolute estimation errors for the IEEE 57-bus system without BD: (a) voltage phase angle error and (b) voltage magnitude error.

To assess the effect of measurement redundancy level on estimation accuracy, two measurement sets are considered: 1) a low redundancy case (L): voltage and power injection measurements at 90 percent of all buses, power flows across all branches ("from" terminal only), and the same PMU placement configurations as in [4]; and 2) a high redundancy level (H): power flows at both terminal nodes of all branches, voltage magnitudes and power injections at all buses, and one more PMU added at a randomly selected bus. In the low redundancy case, the voltage and power injection measurements are distributed evenly across the system. Table IV depicts the mean errors of voltage phase angle and magnitude calculated for all

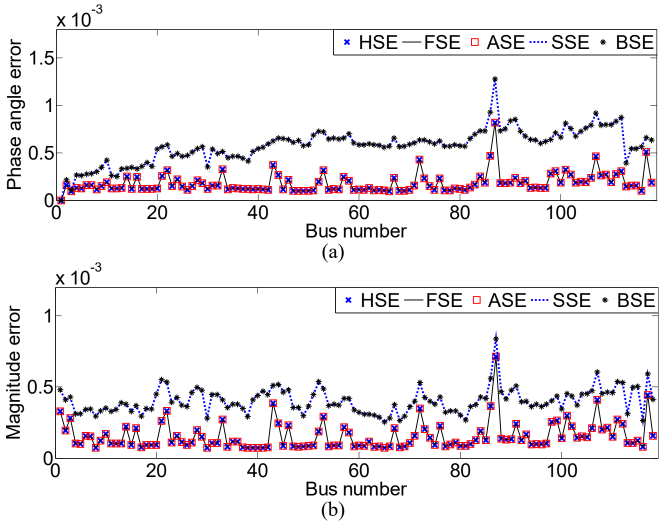

Fig. 5. Absolute estimation errors for the IEEE 118-bus system without BD: (a) voltage phase angle error and (b) voltage magnitude error.

estimators at two measurement redundancy levels. As expected, the estimation errors are lower for the higher redundancy level. Moreover, the SSE and BSE only use the inaccurate SCADA measurements, so their mean estimation errors are larger than those of the other three estimators. Compared to SSE, accuracy of the BSE strategy may deteriorate with a decrease in SCADA measurement redundancy level. However, the numerical indices computed for the five networks demonstrate the same accuracy performance as the FSE and HSE strategies at two measurements redundancy levels. In addition, as described in [13], the ASE can provide estimates with the same accuracy as those obtained by the HSE strategy.

TABLE IV
ACCURACY PERFORMANCE OF FIVE ESTIMATORS

Test system		Error mean	HSE	FSE	ASE	SSE	BSE
IEEE 14-bus	L	$\|V\|$	0.238	0.238	0.238	0.793	0.794
		θ	0.203	0.203	0.203	0.743	0.743
	H	$\|V\|$	0.141	0.141	0.141	0.663	0.663
		θ	0.150	0.150	0.150	0.608	0.608
IEEE 30-bus	L	$\|V\|$	0.245	0.245	0.245	0.747	0.748
		θ	0.262	0.262	0.262	0.971	0.971
	H	$\|V\|$	0.183	0.183	0.183	0.652	0.652
		θ	0.186	0.186	0.186	0.718	0.718
IEEE 57-bus	L	$\|V\|$	0.175	0.175	0.175	0.685	0.686
		θ	0.201	0.201	0.201	0.839	0.839
	H	$\|V\|$	0.154	0.154	0.154	0.576	0.576
		θ	0.166	0.166	0.166	0.647	0.647
IEEE 118-bus	L	$\|V\|$	0.164	0.164	0.164	0.401	0.401
		θ	0.188	0.188	0.188	0.615	0.615
	H	$\|V\|$	0.141	0.141	0.141	0.339	0.338
		θ	0.164	0.164	0.164	0.426	0.426
IEEE 300-bus	L	$\|V\|$	0.262	0.262	0.262	0.516	0.516
		θ	0.482	0.482	0.482	1.147	1.147
	H	$\|V\|$	0.204	0.204	0.204	0.414	0.414
		θ	0.403	0.403	0.403	0.844	0.844

All results are $\times 10^{-3}$.

The absolute estimation errors of the five estimators when four bad SCADA measurements in the PMU-observable area are introduced in the IEEE 30-bus test system are shown in Fig. 6. Compared to the voltage phase angle and magnitude errors of SSE without BD, the accuracy performance of the SSE and BSE deteriorate at different levels due to the bad SCADA measurements. However, because these BD are located in the PMU-observable area, the results achieved by the HSE, FSE, and ASE strategies are barely distinguishable from the best one, i.e., HSE without BD.

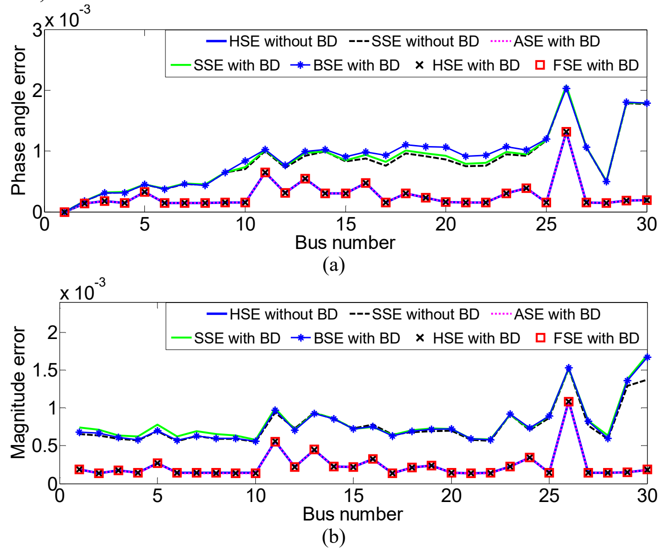

Fig. 6. Absolute estimation errors for the IEEE 30-bus system with four bad SCADA measurements in the PMU-observable area: (a) voltage phase angle error and (b) voltage magnitude error.

Furthermore, the voltage phase angle and magnitude errors derived from five estimators when four bad SCADA measurements (voltage magnitudes V_1 and V_5, active power flow $P_{3\text{-}4}$, and active power injection P_{13}) in the PMU-unobservable area are introduced in the IEEE 30-bus system are depicted in Fig. 7. Similar to what was observed in Fig. 6, the SSE and BSE strategies cannot eliminate the detrimental effect of BD. As shown in Fig. 7(a), the phase angle estimate of bus 13 computed from HSE, FSE, and ASE cannot achieve the same accuracy level when no BD occurs because of the bad active power injection measurement P_{13} located in PMU-unobservable area.

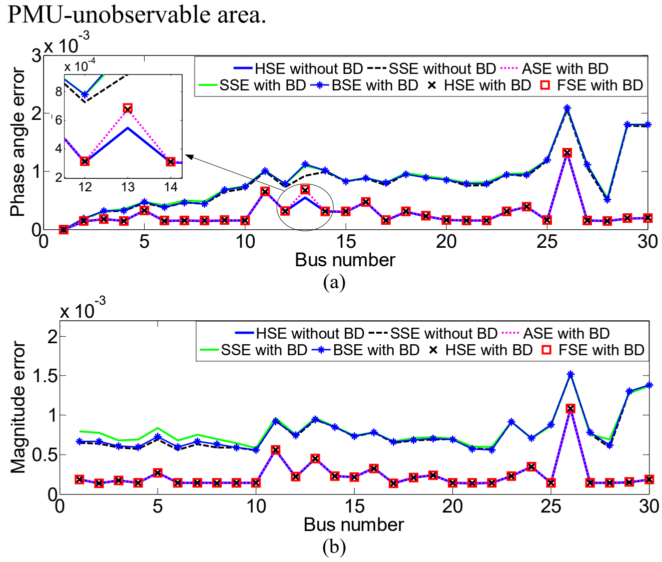

Fig. 7. Absolute estimation errors for the IEEE 30-bus system with four bad SCADA measurements in the PMU-unobservable area: (a) voltage phase angle error and (b) voltage magnitude error.

The absolute estimation errors of three estimators when four PMU measurements (both the phase angles and magnitudes of voltage phasor $\vec{V}_6$ and current phasor $\vec{I}_{6-8}$) are introduced in the 30-bus system are shown in Fig. 8. As shown in Fig. 1, the bad PMU measurements are deleted rather than corrected after being identified. Thus, the originally PMU observable states, i.e., the voltage phase angle and magnitude of bus 8, become unobservable after deleting $\vec{V}_6$ and $\vec{I}_{6-8}$. For this reason, the voltage phase angle and magnitude errors of bus 8 derived from the HSE, ASE, and FSE strategies are much larger than those obtained with no bad PMU measurements.

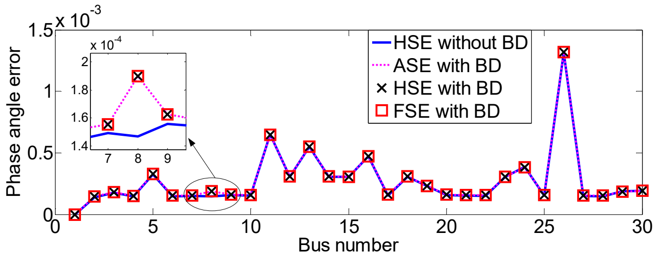

(a)

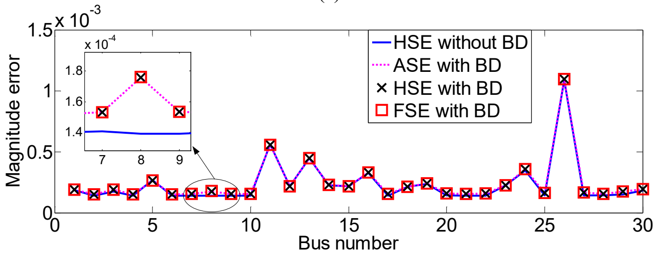

(b)

Fig. 8. Absolute estimation errors for IEEE 30-bus system with four bad PMU measurements: (a) voltage phase angle error and (b) voltage magnitude error.

In summary, the results presented so far demonstrate that the proposed FSE strategy has almost the same estimation accuracy as HSE and ASE strategies for different BD scenarios.

B. Assessment of Computational Effort

All five estimators mentioned in Section III-A were coded in a MATLAB R2013a environment, and carried out on a 3.3-GHz desktop with 4 GB memory. Except for sparse matrix methods, no special effort was made to optimize the program codes. For each test system, the proposed FSE was assessed by comparing it with the other estimators in terms of computing time under five cases:

- Case 1: No BD;
- Case 2: Five BD in SCADA measurements (all of these BD are in the PMU-observable area);
- Case 3: Five BD in SCADA measurements (three BD are in the PMU-observable area and two BD are in the PMU-unobservable area);
- Case 4: Five BD in SCADA measurements (all of these BD are in the PMU-unobservable area); and
- Case 5: Four BD, i.e., two bad voltage/current phasor measurements (both their phase angle and magnitude) in PMU measurements.

In each case, 100 Monte Carlo simulations were executed with different Gaussian errors, and BD values were assigned to different measurements in each simulation run. The BD detection threshold adopted in this study for normalized residual tests is 3, i.e., 99.7% confidence level. Because the PMU-based estimator and the first stage of the SCADA-based estimator constitute separate modules and process distinct measurement sets, it is reasonable to consider a parallelization of these two processes (Fig. 1). Accordingly, if t_{PMU}, t_{fusion}, t_1, t_2, and t_3 denote the execution time of PMU-based SE, fusion stage, and the first, second, and third stages of SCADA-based SE, respectively, then the computing time for the FSE strategy, t_{FSE}, can be derived as follows:

$$t_{FSE} = \max(t_1, t_{PMU}) + t_2 + t_3 + t_{fusion} \quad (63)\#$$

Table V provides the computing time for each individual stage of the FSE strategy as well as the total execution time for Case 1. For the IEEE 14-bus and 30-bus systems, although the PMU-based SE and the first stage of SCADA-based SE are both linear, and a larger number of measurements are processed in the latter, $t_{PMU} > t_1$ due to the additional calculation of the PMU measurement vector in rectangular coordinates as well as its error covariance matrix. With growing network size, t_1 increases considerably and even takes up a much larger proportion in t_{FSE}; this is expected due to the sharp rise in the number of SCADA measurements.

TABLE V
COMPUTING TIME (MS) FOR FSE STRATEGY WITHOUT BD

Test System	t_1	t_{PMU}	t_2	t_3	t_{fusion}	t_{FSE}
IEEE 14-bus	0.3	0.6	0.26	0.26	0.4	1.52
IEEE 30-bus	0.7	1.1	0.5	0.5	0.8	2.9
IEEE 57-bus	3.0	2.9	0.5	0.8	2.1	6.4
IEEE 118-bus	16.2	3.9	0.7	1.7	8.2	26.8
IEEE 300-bus	51.8	26.2	1.2	9.6	91.3	153.9

Table VI presents the computing time of five estimators under five cases for each test system, in which t_{HSE}, t_{FSE}, t_{ASE}, t_{SSE}, and t_{BSE} represent the execution times of the HSE, FSE, ASE, SSE, and BSE strategies, respectively. The SSE and BSE use only SCADA measurements. When there are no BD (Case 1), the speedup achieved by BSE, defined as t_{SSE}/t_{BSE}, ranges from 2.7 to 3.8, with higher values obtained for larger networks. The speedup values, ranging from 3.6 to 5.4, are obtained when five BD occur in the SCADA measurements (Cases 2-4). This can be explained as follows: although BD in these two estimators are identified and corrected one-by-one, the re-estimation step in BSE is linear and can significantly reduce the required computing time. The other three estimators, i.e., HSE, FSE, and ASE, deal with both SCADA and PMU measurements. The proposed FSE methodology has superior computational performance, resulting in up to 3.4~4.7 and 1.8~2.8 orders of implementation time reduction compared to HSE and ASE, respectively, for the five test systems under Case 1. For the cases with bad measurements, the resulting speedups, defined as t_{HSE}/t_{FSE} and t_{ASE}/t_{FSE}, are remarkably high (from 4.9 to 14.2 and 2.0 to 6.5, respectively). In Case 4, all five bad SCADA measurements are in the PMU-unobservable area, so these BD are identified and eliminated one-by-one in the FSE. On the contrary, the same amount of BD in Case 2 can be dealt with all at once, and is why the computing time of the FSE for Case 2 is much less than for Case 4. Before BD processing, the estimates derived from the HSE for Case 2 are more accurate than for Case 4 because the detrimental effect of bad SCADA measurements in the PMU-observable area is weakened by the accurate PMU measurements. Moreover, a hot-start execution is implemented in the re-estimation step of BD processing for the HSE solution. Thus, compared to Case 4, the average number of iterations in the re-estimation step in Case 2 can be significantly reduced, and its execution time decreases accordingly. However, for each test system, the ASE solution in Cases 2-4 takes almost the same execution time. In addition to dealing with a smaller BD set, HSE and FSE in Case 5 omit the BD correction step, which gives rise to a shorter implementation time than for Cases 2-4. It is worth mentioning that the execution time of ASE in Case 5 is about 2.5-fold less compared to Cases 2-4 for the five test systems because the re-estimation step in the former case is non-iterative.

TABLE VI
COMPUTATIONAL EFFORT OF FIVE ESTIMATORS UNDER FIVE CASES

Test System	Case	Computing Time (ms)				
		t_{HSE}	t_{FSE}	t_{ASE}	t_{SSE}	t_{BSE}
IEEE 14-bus	1	5.20	1.52	2.81	2.20	0.82
	2	19.3	3.1	13.4	12.7	3.4
	3	22.9	3.6	13.3	12.5	3.5
	4	25.5	4.0	13.4	12.6	3.5
	5	17.7	2.7	5.4	-	-
IEEE 30-bus	1	10.3	2.9	5.3	4.6	1.7
	2	42.3	5.2	32.1	30.5	8.3
	3	45.7	8.1	31.7	30.4	8.4
	4	48.3	9.9	32.0	30.5	8.4
	5	40.8	4.8	12.7	-	-
IEEE 57-bus	1	27.6	6.4	15.4	11.7	4.3
	2	113.1	14.1	88.5	84.8	23.2
	3	133.3	20.6	88.4	84.5	23.5
	4	143.6	25.3	88.4	84.7	23.3
	5	109.2	11.6	34.8	-	-
IEEE 118-bus	1	122.1	26.8	75.1	57.5	18.6
	2	526.1	60.4	389.8	373.0	78.8
	3	580.3	78.6	390.0	372.5	78.6
	4	622.5	86.8	389.5	372.4	78.7
	5	507.9	35.7	151.6	-	-
IEEE 300-bus	1	720.9	153.9	397.4	241.0	62.6
	2	2809.2	348.2	2160.2	2003.5	373.6
	3	3056.2	372.0	2159.8	2002.8	372.8
	4	3298.5	396.5	2160.1	2003.2	374.1
	5	2589.8	193.1	850.2	-	-

To further demonstrate the superiority of computational performance of the proposed FSE, the average number of megaflops (floating-point operations × 10^6) of five estimators under five cases for IEEE 30- and 118-bus systems are calculated using a FLOPs counter [26] and depicted in Table VII. Compared to SSE, the linear re-estimation step in BSE leads to a significant reduction in the number of megaflops. Moreover, the number of megaflops required by ASE increases rapidly in the presence of five bad SCADA measurements. In addition, comparing megaflops in Cases 1 and 5 shows that the bad PMU measurements have a far greater impact on the computational effort for HSE than for FSE, with a 3- to 4-fold megaflops increase for HSE and only a very small increase for FSE. This is because the bad PMU measurements with large weights can seriously affect the accuracy of the estimates obtained from HSE before BD processing and the required iteration number in the following re-estimation step will be sharply increased, while bad PMU measurements in FSE can be eliminated all at once. It is worth mentioning that, as shown in Table VI, the computing time of FSE in Case 2 for IEEE 30- or 118-bus systems is almost equal to or less than that of ASE and SSE in Case 1, but the corresponding megaflops illustrated in Table VII almost triple. This demonstrates the parallelism degree of the proposed FSE strategy is higher than that of ASE and SSE. Thus, FSE can take more advantage of the high performance parallel processors (e.g., field-programmable gate arrays [27] and graphics processing units [28]) that have experienced rapid development in the past few years.

TABLE VII
NUMBER OF MEGAFLOPS OF FIVE ESTIMATORS UNDER FIVE CASES

Test System	Case	Number of Megaflops				
		HSE	FSE	ASE	SSE	BSE
IEEE 30-bus	1	89.4	13.6	20.4	14.6	10.2
	2	401.4	51.3	269.1	263.3	40.8
	3	445.8	57.4	269.1	263.3	40.8
	4	468.1	45.9	269.1	263.3	40.8
	5	371.6	14.4	40.7	-	-
IEEE 118-bus	1	6715	979	1630	1348	818
	2	22888	3944	13625	13344	3107
	3	25570	4421	13625	13344	3107
	4	28251	3835	13625	13344	3107
	5	20464	1008	2661	-	-

IV. CONCLUSIONS

In this paper, we present a fast algorithm for combining SCADA and insufficient PMU measurements in state estimation. Five test systems, i.e., IEEE 14-bus, 30-bus, 57-bus, 118-bus and 300-bus systems, are employed to assess the proposed estimator under various BD scenarios. Simulation results show that the proposed estimator takes much less computing time compared to existing approaches, especially for large-scale networks with multiple bad SCADA measurements in the PMU-observable area, and can provide almost the same estimation accuracy as the HSE estimator.

REFERENCES

[1] F. C. Schweppe and J. Wildes, “Power system static-state estimation, part I, II, III,” *IEEE Trans. Power App. Syst.*, vol. PAS-89, no. 1, pp. 120-135, Jan. 1970.

[2] A. Abur and A. G. Expósito, *Power System State Estimation Theory and Implementation*. New York: Marcel Dekker, 2004.

[3] A. G. Phadke and J. S. Thorp, *Synchronized Phasor Measurements and Their Applications*. New York: Springer, 2008.

[4] N. Kashyap, S. Werner, Y-F. Huang, and T. Riihonen, “Power system state estimation under incomplete PMU observability - a reduced-order approach,” *IEEE J. Sel. Topics Signal Process.*, vol. 8, no. 1, pp. 1051-1062, Dec. 2014.

[5] G. Valverde, S. Chakrabarti, E. Kyriakides, and V. Terzija, “A constrained formulation for hybrid state estimation,” *IEEE Trans. Power Syst.*, vol. 26, no. 3, pp. 1102-1109, Aug. 2011.

[6] A. S. Costa, A. Albuquerque, and D. Bez, “An estimation fusion method for including phasor measurements into power system real-time modeling,” *IEEE Trans. Power Syst.*, vol. 28, no. 2, pp. 1910-1920, May 2013.

[7] M. B. Do Coutto Filho, J. C. S. de Souza, and M. A. R. Guimaraens, “Enhanced bad data processing by phasor-aided state estimation,” *IEEE Trans. Power Syst.*, vol. 29, no. 5, pp. 2200-2209, Sep. 2014.

[8] M. Göl and A. Abur, “A hybrid state estimator for systems with limited number of PMUs,” *IEEE Trans. Power Syst.*, vol. 30, no. 3, pp. 1511-1517, May 2015.

[9] T. S. Bi, X. H. Qin, and Q. X. Yang, "A novel hybrid state estimator for including synchronized phasor measurements," *Elect. Power Syst. Res.*, vol. 78, no. 8, pp. 1343-1352, 2008.
[10] G. N. Korres and N. M. Manousakis, "State estimation and bad data processing for systems including PMU and SCADA measurements," *Elect. Power Syst. Res.*, vol. 81, no. 7, pp. 1514-1524, 2011.
[11] G. N. Korres and N. M. Manousakis, "A state estimator including conventional and synchronized phasor measurements," *Comput. Electrical Eng.*, vol. 38, no. 2, pp. 294-305, 2012.
[12] S. Chakrabarti, E. Kyriakides, G. Ledwich, and A. Ghosh, "Inclusion of PMU current phasor measurements in a power system state estimator," *IET Gen., Transm., Distrib.*, vol. 4, no. 10, pp. 1104-1115, 2010.
[13] M. Zhou, V. A. Centeno, J. S. Thorp, and A. G. Phadke, "An alternative for including phasor measurements in state estimators," *IEEE Trans. Power Syst.*, vol. 21, no. 4, pp. 1930-1937, Nov. 2006.
[14] L. Zhao and A. Abur, "Multiarea state estimation using synchronized phasor measurements," *IEEE Trans. Power Syst.*, vol. 20, no. 2, pp. 611-617, May 2005.
[15] R. Baltensperger, A. Loosli, H. Sauvain, M. Zima, G. Andersson, and R. Nuqui, "An implementation of two-stage hybrid state estimation with limited number of PMU," in *Proc. 10th IET Int. Conf. Developments in Power Syst. Protection*, Mar. 2010, pp. 1–5.
[16] N. M. Manousakis, G. N. Korres, J. N. Aliprantis, G. P. Vavourakis, and G.-C. J. Makrinas, "A two-stage state estimator for power systems with PMU and SCADA measurements," in *Proc. IEEE Grenoble PowerTech (POWERTECH)*, Grenoble, France, Jun. 2013, pp. 1–6.
[17] W. Q. Jiang, V. Vittal, and G. T. Heydt, "A distributed state estimator utilizing synchronized phasor measurements," *IEEE Trans. Power Syst.*, vol. 22, no. 2, pp. 563-571, May 2007.
[18] W. Q. Jiang, V. Vittal, and G. T. Heydt, "Diakoptic state estimation using phasor measurement units," *IEEE Trans. Power Syst.*, vol. 23, no. 4, pp. 1580-1589, Nov. 2008.
[19] T. Yang, H. Sun, and A. Bose, "Transition to a two-level linear state estimator-part I: architecture," *IEEE Trans. Power Syst.*, vol. 26, no. 1, pp. 46-53, Feb. 2011.
[20] T. Yang, H. Sun, and A. Bose, "Transition to a two-level linear state estimator-part II: algorithm," *IEEE Trans. Power Syst.*, vol. 26, no. 1, pp. 54-62, Feb. 2011.
[21] A. Gómez-Expósito, C. Gómez-Quiles, and A. de la Villa Jaén, "Bilinear power system state estimation," *IEEE Trans. Power Syst.*, vol. 27, no. 1, pp. 493-501, Feb. 2012.
[22] A. de la Villa, C. Gómez-Quiles, and A. Gómez-Expósito, "A factorized approach to WLS state estimation," *IEEE Trans. Power Syst.*, vol. 26, no. 3, pp. 1724-1732, Aug. 2011.
[23] T. Van Cutsem, M. Ribbens-Pavella, and L. Mili, "Hypothesis testing identification: A new method for bad data analysis in power system state estimation," *IEEE Trans. Power App. Syst.*, vol. PAS-100, no. 11, pp. 3239-3252, Nov. 1984.
[24] J. Chen and A. Abur, "Placement of PMUs to enable bad data detection in state estimation," *IEEE Trans. Power Syst.*, vol. 21, no. 4, pp. 1608–1615, Nov. 2006.
[25] MATPOWER: A MATLAB Power System Simulation Package [Online]. Available: http://www.pserc.cornell.edu/matpower/.
[26] H. Qian, "User guide for FLOPS," pp. 1-7, Apr. 2015: http://www.mathworks.com/matlabcentral/fileexchange/50608-counting-the-floating-point-operations--flops-.
[27] A. Cardenas, C. Guzman, and K. Agbossou, "Development of a FPGA based real-time power analysis and control for distributed generation interface," *IEEE Trans. Power Syst.*, vol. 27, no. 3, pp. 1343-1353, Aug. 2012.
[28] V. Jalili-Marandi and V. Dinavahi, "SIMD-based large-scale transient stability simulation on the graphics processing unit," *IEEE Trans. Power Syst.*, vol. 25, no. 3, pp. 1589-1599, Aug. 2010.

Ting Wu (S'14) received the B.Eng. degree in automation from Central South University, Changsha, China, in 2010, the M. Eng. Degree in Control Theory and Control Engineering from Zhejiang University, Hangzhou, China, in 2013, and the Ph.D. degree from The Hong Kong Polytechnic University, Hong Kong, China, in 2017.

She is currently a Lecturer in the College of Information Engineering, Zhejiang University of Technology, Hangzhou, China. Her research interests include PMUs, wide-area monitoring and control, and state estimation.

C. Y. Chung (M'01-SM'07-F'16) received B.Eng. (with First Class Honors) and Ph.D. degrees in electrical engineering from The Hong Kong Polytechnic University, Hong Kong, China, in 1995 and 1999, respectively.

He has worked for Powertech Labs, Inc., Surrey, BC, Canada; the University of Alberta, Edmonton, AB, Canada; and The Hong Kong Polytechnic University, China. He is currently a Professor, the NSERC/SaskPower (Senior) Industrial Research Chair in Smart Grid Technologies, and the SaskPower Chair in Power Systems Engineering in the Department of Electrical and Computer Engineering at the University of Saskatchewan, Saskatoon, SK, Canada. His research interests include smart grid technologies, renewable energy, power system stability/control, planning and operation, computational intelligence applications, and power markets.

Dr. Chung is an Editor of *IEEE Transactions on Sustainable Energy* and an Associate Editor of *IET Generation, Transmission, and Distribution*. He is also a Member-at-Large (Global Outreach) of the IEEE PES Governing Board.

Innocent Kamwa (S'83-M'88-SM'98-F'05) received a Ph.D. from Laval University, QC, Canada, in 1988. He then joined Hydro-Québec's Research Institute (IREQ), Varennes, Canada, where he is currently Project Manager of Power Grid Control and Automation and the Chief Scientist of Hydro-Québec's Smart Grid. He is a Professional Engineer and an Adjunct Professor of Power Systems Engineering with McGill University and Laval University.

Dr. Kamwa serves on many IEEE/PES technical committees as a member and an officer, including the Fellow Evaluation, Electric Machinery, and Power System Stability committees. Dr. Kamwa is an Editor of *IEEE Transactions on Power Systems* and the Co-Editor-in-Chief of *IET Generation, Transmission and Distribution*. He was a recipient of the IEEE PES Prize Paper Award in 1998, 2003, and 2009.